pH-labile PEGylation of siRNA-loaded lipid nanoparticle improves active targeting and gene silencing activity in hepatocytes

Kazuki Hashiba,† Yusuke Sato,† Hideyoshi Harashima⋆

Faculty of Pharmaceutical Sciences, Hokkaido University, Kita 12 Nishi 6, Kita-ku, Sapporo 060-0812, Japan

†These authors are contributed equally to this work.

⋆Corresponding author

Hideyoshi Harashima, PhD
Faculty of Pharmaceutical Science
Hokkaido University
Kita-12 Nishi-6, Kita-ku, Sapporo, Hokkaido, 050-0812, Japan.
Tel.: +81 11 706 3919
Fax: +81 11 706 3734
E-mail: harasima@pharm.hokudai.ac.jp

Abstract

Lipid nanoparticles (LNPs) are one of the promising technologies for the *in vivo* delivery of short interfering RNA (siRNA). Modifying LNPs with polyethyleneglycol (PEG) is widely used to inhibit non-specific interactions with serum components in the blood stream, and is a useful strategy for maximizing the efficiency of active targeting. However, it is a widely accepted fact that PEGylation of the LNP surface strongly inhibits fusion between LNPs and endosomal membranes, resulting in poor cytosolic siRNA delivery, a process that is referred to as the 'PEG-dilemma'. In the present study, in an attempt to overcome this problem, siRNA-loaded LNPs were modified with PEG through maleic anhydride, a pH-labile linkage. The *in vitro*, suppression of cationic charge, stealth function at physiological pH up to 1 hour and the rapid desorption of PEG and restoration of fusogenic activity under slightly acidic conditions (within only 2 min) were achieved by PEG modification of the LNPs through maleic anhydride. *In vivo*, PEG modification through maleic anhydride resulted in a dramatic improvement in the targeting capability of the active targeting of ligand (*N*-acetyl-D-galactosamine)-modified LNPs to hepatocytes, with an approximately 14-fold increase in gene silencing activity in factor 7 model mice. Taken together, the maleic anhydride-mediated pH-labile PEGylation of the active targeting LNPs is a useful strategy for achieving the specific and efficient delivery of siRNAs *in vivo*.

Key words

Maleic anhydride, pH-labile, PEGylation, siRNA delivery, Active target, Lipid nanoparticles

1. Introduction

Since the discovery of short interfering RNA (siRNA) [1], which induces specific gene silencing through RNA interference (RNAi) [2], the focus of many researchers has been on realizing RNAi-based medicine for treating refractory diseases. Because of the characteristics of siRNA, which include hydrophilicity, a negative charge and high molecular weight, adequate delivery technology is essential for improving the bioavailability of siRNA.

Active targeting is a useful strategy for achieving the cell-specific delivery of payloads. Basically, active targeting involves the use of an appropriate ligand that recognizes the target cells. However, specific delivery sometimes cannot be achieved because of non-specific interactions of the vehicle used with biomolecules and elimination from the blood circulation by the reticuloendothelial system (RES), resulting in a decreased efficiency for ligand-mediated specific delivery to target cells. Therefore, minimization of non-specific recognition by RES is important to maximize the efficiency of an active targeting agent.

Polyethyleneglycol (PEG) modification (PEGylation) is an accepted strategy for inhibiting non-specific recognition by RES [3, 4]. PEGylation of the surface of nanoparticle results in formation of a fixed aqueous layer, which inhibits the adsorption of serum proteins through electrostatic and hydrophobic interactions [5]. However, after internalization into target cells, the aqueous layer also strongly inhibits interactions of the nanoparticles with the endosomal membrane, which reduces the efficiency of cytosolic delivery of the cargo. This issue is sometimes referred to as the PEG-dilemma [6-8].

Many kinds of strategies have been developed to overcome the PEG-dilemma. One such strategy is the environment-responsive removal of the PEG from nanoparticles inside and/or outside of the target cells [7]. Among the various environments, the difference in pH between the blood circulation and endosomes/lysosomes is one of the most extensively investigated factors. PEGylation through a pH-labile linkage, such as an acetal, orthoester and hydrazone, is a useful strategy for adding a pH-sensitive functionality [9-14]. However, While, in most studies, the pH-sensitive functionalities of these pH-labile linkages were examined *in vitro*, information concerning the pH-labile linkages *in vivo* is much less extensive. In addition, among these pH-labile linkages, a maleic anhydride derivative has some advantages including that the modification can be done in water and that fact that a pH-sensitivity of the final product can be controlled by slight modification of the chemical structure. Maleic anhydride

derivatives have been applied only in a few polymer-based siRNA delivery systems but not in siRNA-loaded lipid nanoparticles (LNPs) [15-17].

LNPs are one of the promising systems for delivering siRNA [18-22]. As the result of the recent development of novel cationic lipids by rational design and combinatorial screening approaches, the efficiency of siRNA delivery has been dramatically improved, especially in liver tissues [23-27].

In the present study, we report on the development of siRNA-loaded LNPs for targeting hepatocytes using a hepatotropic ligand, *N*-acetyl-D-galactosamine (GalNAc) [28, 29] and modifying the LNPs with maleic anhydride. The use of maleic anhydride for PEG-modification resulted in a significant improvement in the hepatocyte targeting efficiency of the GalNAc-modified LNPs and in an improvement in factor 7 (F7) gene silencing activity. F7 gene silencing activity was further improved by optimizing the structure of the maleic anhydride (14-fold higher activity compared to that of the GalNAc-LNPs without PEGylation through maleic anhydride). These findings suggest that the strategy that involves a combination of a specific ligand and pH-labile PEG shielding would be useful for improving the active targeting efficiency of LNPs for siRNA delivery *in vivo*.

2. Materials and methods

2.1 Materials

1,2-Dioleoyl-*sn*-glycerol-3-phosphatidylserine (DOPS), 1,2-dioleoyl-*sn*-glycero-3-phosphatidylcholine (DOPC) and 1,2-dimyristoyl-*sn*-glycerol methoxypolyethylene glycol (DMG-$_{m}$PEG$_{2k}$) were purchased from NOF Corporation (Tokyo, Japan). Cholesterol (chol), 1,2-Dioleoyl-*sn*-glycero-3-phosphoethanolamine-*N*-(7-nitro-2-1,3-benzoxadiazol-4-yl) (NBD-DOPE) and 1,2-dioleoyl-*sn*-glycero-3-phsphoethanolamine-*N*-(lissamine rhodamine B sulfonyl) (Rho-DOPE) were purchased from Avanti Polar Lipids (Alabster, AL). Carboxylated dimethylmaleic anhydride (CDM)-$_{m}$PEG$_{2k}$, carboxylated ethylmaleic anhydride (CEM)-$_{m}$PEG$_{2k}$ and chol-PEG$_{400}$-amine were synthesized in our laboratory (Supplementary Information). YSK05 was synthesized as described previously [30]. Trivalent GalNAc ligand was synthesized according to the PCT publication WO 2009/073809. Ribogreen, 3,3′-Dioctadecyloxacarbocyanine perchlorate (DiO) and 1,1'-dioctadecyl-3,3,3',3'-tetramethylindocarbocyanine perchlate (DiI) were purchased from Molecular Proves (Eugene, OR, USA). Sodium 2,4,6-trinitrobenzensulfonate (TNBS) was purchased from Wako Chemicals (Osaka, Japan). FITC-conjugated Isolectin B4 was purchased from Vector Laboratories (Burlingame, CA). All siRNA samples were purchased from Hokkaido System Science Co. Ltd. (Sapporo, Japan). The siF7 sense and antisense strand sequences are 5'-GGAucAucucAAGucuuAcTsT-3' and 5'-GuAAGAcuuGAGAuGAuccTsT-3', respectively. The siGFP-Cy5 sense and antisense strand sequences are 5'-ACAUGAAGCAGCACGACuUTsT-3' and 5'-AAGUCGUGCUGCUUCAUGUTsT-Cy5-3', respectively. 2'-Fluoro-modified nucleotides represented in lower case, phosphorothioate linkage represented as s.

2.2 Animals

Female ICR mice, 4 weeks of age, were purchased from Japan SLC (Shizuoka, Japan). The experimental protocols were reviewed and approved by the Hokkaido University Animal Care Committee in accordance with the guidelines for the care and use of laboratory animals.

2.3 Preparation of LNPs

A 90% *t*-BuOH solution containing YSK05/chol/chol-PEG$_{400}$-amine/DMG-$_{m}$PEG$_{2k}$ at a molar ratio of 70/30/15/1.5 were prepared at a concentration of 7.5 mM total lipid. In case of GalNAc modification, 0.25 to 0.5 mol% of trivalent GalNAc ligand was added

to the above solution. These lipid solutions were mixed with 0.4 mg/mL siRNA solution to be N/P ratio of 8. LNPs were prepared by gradually adding this mixture to 20 mM Citrate buffer (pH4.0) under vigorous mixing. The resulting LNP solution were diluted with 0.1 M HEPES buffer (pH9.5) and ultrafiltrated using Vivaspin Turbo-15 (MWCO 100 kDa, Sartorius) twice for removal of *t*-BuOH, adjustment of pH. The size and ζ-potential of the LNPs were measured by a Zetasizer Nano ZS ZEN3600 instrument (Malvern Instruments, Worcestershire, UK). The encapsulation efficiency and total concentration of siRNA were measured by a Ribogreen assay, as described previously [30].

2.4 Modification of LNPs with maleic anhydride derivatives

To modify the LNPs with maleic anhydride derivatives, LNPs at a concentration of 10 mM total lipid suspended in 0.1 M HEPES buffer (pH9.5) was added to a dried powder of various (0 to 2.5) equivalents of CDM-$_{m}$PEG$_{2k}$ or CEM-$_{m}$PEG$_{2k}$. The modified LNPs were preserved at 4˚C until used in experiments.

2.5 Measurement of the efficiency of maleic anhydride modification

The efficiency of surface modification was measured by detecting remaining primary amino groups using TNBS. The modified LNP solution was diluted with 0.1 M borate buffer (pH9.5) dissolving 0.4 mM TNBS and incubated for 30 min at 25˚C with gentle shaking (700 rpm). After the incubation, TritonX-100 was added to a final TritonX-100 concentration of 1.0 w/v%, and the absorbance at 420 nm was then measured and normalized by unmodified LNPs.

2.6 Measurement of hydrolysis rate

The rate of hydrolysis maleic acid amide was measured by detecting primary amino group using TNBS. Maleic anhydride-modified LNPs were diluted with 0.1 M Citrate buffer (pH 4.0), 0.1 M MES buffer (pH 6.0) or 0.1 M HEPES buffer (pH 7.5), and then incubated for the indicated times at 37˚C with gentle shaking (700 rpm). After the incubation, each LNPs was diluted with 0.1 M borate buffer (pH 10) dissolving 0.4 mM TNBS, and was incubated for 30 min at 25˚C with gentle shaking (700 rpm). After the incubation, this mixture were added with TritonX-100 to be a final TritonX-100 concentration 0.5 w/v%, and then absorbance at 420 nm was measured and normalized by that of unmodified LNPs.

2.7 Measurement of cellular uptake

HeLa cells stably expressing Firefly and Renilla luciferase (HeLa-dluc) were cultured in cell-culture dishes (Corning) containing DMEM supplemented with 10% FBS, penicillin (100 U/mL), streptomycin (100 μg/mL) and G418 (0.4 mg/mL) at 37˚C in 5% CO_2. HeLa-dluc cells were seeded at 1.0×10^5 cells per well in 6-well plates in growth media 24 hr prior to transfection. The LNPs were diluted with growth media to reach 10 nM siRNA and added to the cells after the aspiration of spent media. The cells were washed with PBS(-) twice at the indicated times and collected by trypsin treatment. The cells were centrifuged and, after removing the supernatant, were resuspended with FACS buffer (PBS(-) containing 0.5% bovine serum albumin and 0.02% sodium azide). The cells were filtered through a nylon mesh and measured by FACSCalibur (Becton Dickinson, Franklin Lakes, NJ, USA).

2.8 Measurement of fusogenic activity by fluorescent resonance energy transfer (FRET)

Anionic liposomes containing DOPS/DOPC/NBD-DOPE/ Rho-DOPE at a molar ratio of 70/30/1.0/0.5 were prepared by simple hydration methods. Thirty hundred μL of Anionic liposome at a concentration of 0.25 mM lipid was diluted with 600 μL of MES-HEPES buffer (50 mM MES, 50 mM HEPES, 50 mM NaCl, pH 6.0) and 1800 μL of saline. Thirty hundred μL of LNPs at a concentration of 0.25 mM lipid was added to the solution containing anionic liposomes. The mixture was incubated at 37˚C with stirring and fluorescent derived from Rho-DOPE was measured using a spectrofluorometer (FP-6300) with settings of λ_{ex}=470 nm, λ_{em}=530 nm. The sample added with 300 μL of 10 w/v% TritonX-100 instead of the LNP solution was measured as a positive control.

2.9 Measurement of intrahepatic distribution of LNPs

ICR mice were intravenously injected with DiI (0.5 mol% of total lipid) labeled LNPs, which were diluted with PBS to become an appropriate concentration immediately prior to injection at a dose of 0.5 mg siRNA/kg. One hour after the injection, liver tissues were collected and stained with 20 μg/mL FITC-conjugated Isolectin B4. Intrahepatic distribution of the LNPs was observed using a Nikon A1 (Nikon Co. Ltd. Tokyo, Japan). Images were captured by ×60 objective.

2.10 Measurement of plasma coagulation factor 7 (F7) activity

ICR mice were intravenously injected with the LNPs, which were diluted with PBS(-) to become an appropriate concentration just before injection. Twenty-four hours after

injection, mice were euthanized and blood was collected by cardiac puncture and processed to plasma using heparin. Plasma F7 activity were measured using a Biophen F7 chromogenic assay kit (Aniara Corporation, West Chester, OH, USA) according to manufacturer's protocol.

2.11 Statistical analysis

Results are expressed as the mean±SD. Statistical comparisons between two groups were evaluated by the Student's *t*-test and corrected by ANOVA for multiple comparisons.

3. Results

3.1 Preparation of LNPs

The LNPs used in this study were prepared by the *t*-BuOH dilution method as described previously [30]. The LNPs were composed of pH-sensitive cationic lipid, YSK05 (previously developed in our laboratory [30]), cholesterol and $_{m}PEG_{2k}$-DMG at a molar ratio of 70/30/1.5. In addition, 15 mol% of chol-PEG_{400}-amine was inserted to the LNPs as a donor of primary amino groups which react with maleic anhydride [31]. Modification with the chol-PEG_{400}-amine resulted in an increase in the ζ-potential of the LNPs due to its cationic charge derived from primary amino groups and an approximately a 3-fold improvement in *in vitro* gene silencing activity (Figure S1A, B). The fusogenic activity of the LNPs was evaluated by the cancellation of FRET. As a model of an endosome, an anionic liposome labeled with a FRET pair (NBD-DOPE/Rho-DOPE) was mixed with the LNPs at pH6.0, which mimics the pH in acidic endosomes. Modification with the chol-PEG_{400}-amine resulted in a significant improvement in the fusogenic activity of the LNPs with anionic liposomes (Figure S1C). After the formation of the LNPs, the LNPs were reacted with CDM-$_{m}PEG_{2k}$. The chemical structure of all components used for the LNPs is shown in Figure 1.

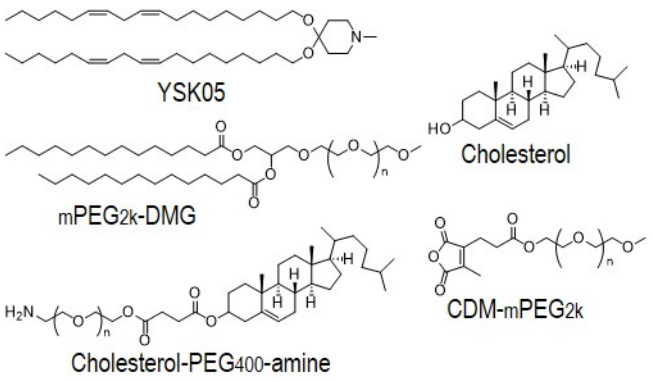

Figure 1 Chemical structure of the LNP components used in this study.

In a preliminary experiment, the amount of the CDM-$_{m}PEG_{2k}$ against the LNPs was examined from 0 to 2.5 equivalence. The ζ-potential of the LNPs gradually decreased as a function of the equivalence of CDM-$_{m}PEG_{2k}$, reaching approximately -15 mV at 2.5 equivalence (Figure 2A). The decrease in ζ-potential of the LNPs results from both a decrease in primary amino groups and the production of carboxyl groups through reactions between primary amino groups and CDM. A TNBS assay revealed that the

reaction rate reached approximately 50% at a 2.5 equivalence (Figure 2B). Particle size and siRNA encapsulation rate were not affected by the reaction (Figure 2C, D).

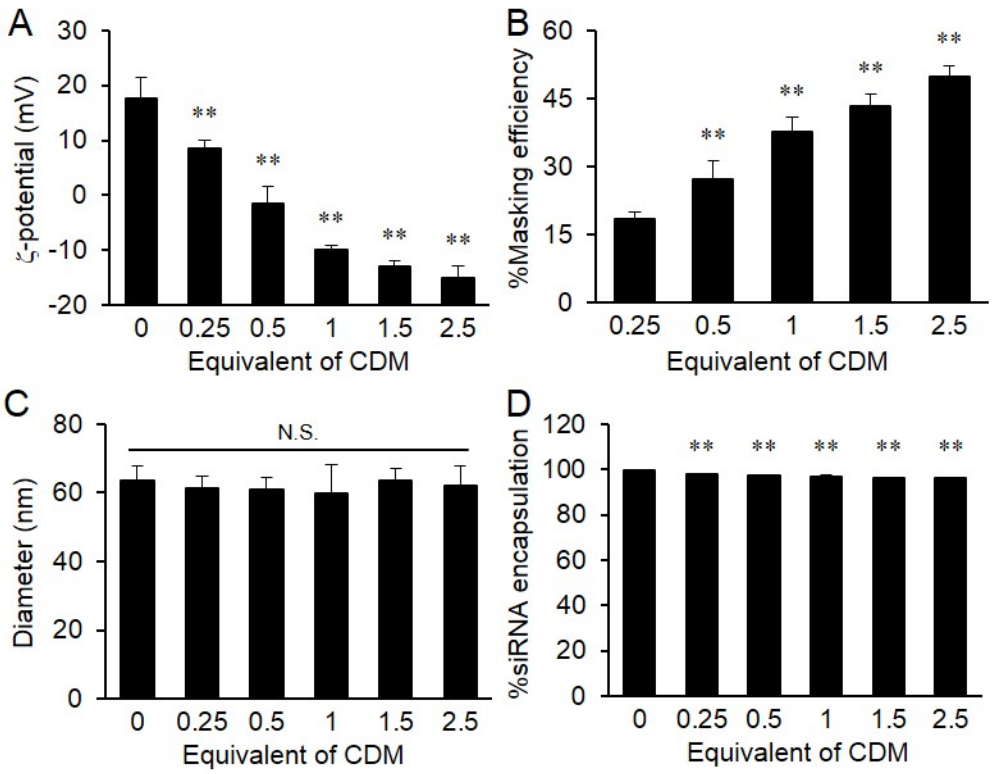

Figure 2 Properties of the LNPs before and after modification with CDM-$_m$PEG$_{2k}$. (A) ζ-potentials of the LNPs. (B) Masking efficiency was measured by a TNBS assay. (C) Mean diameter of the LNPs. (D) siRNA encapsulation ratio quantified by Ribogreen assay. n=3. Data are represented as the mean±SD. n=3. **P<0.01 (by one-way nrANOVA, followed by the Dunnett test. (A, C, D) vs. 0 equivalent of CDM. (B) vs.0.25 equivalent of CDM). N.S.: not significant.

3.2 *In vitro* evaluation of transient stealth function by modification with CDM-$_m$PEG$_{2k}$

To confirm the transient stealth function resulting from modification with CDM-$_m$PEG$_{2k}$, the cellular uptake of the LNPs was measured. Two types of fluorescent probes, DiO and Cy5, were used to trace the LNP lipids and siRNAs, respectively. At an early time (30 min), modification with CDM-$_m$PEG$_{2k}$ resulted in significantly lower cellular uptake (Figure 3). On the other hand, at a later time (2 hours), the cellular uptake of the LNPs with and without CDM-$_m$PEG$_{2k}$ modification (expressed as CDM(+) and CDM(-), respectively) was comparable (Figure 3). This result indicates that modification with CDM-$_m$PEG$_{2k}$ confers a transient stealth function to the LNPs.

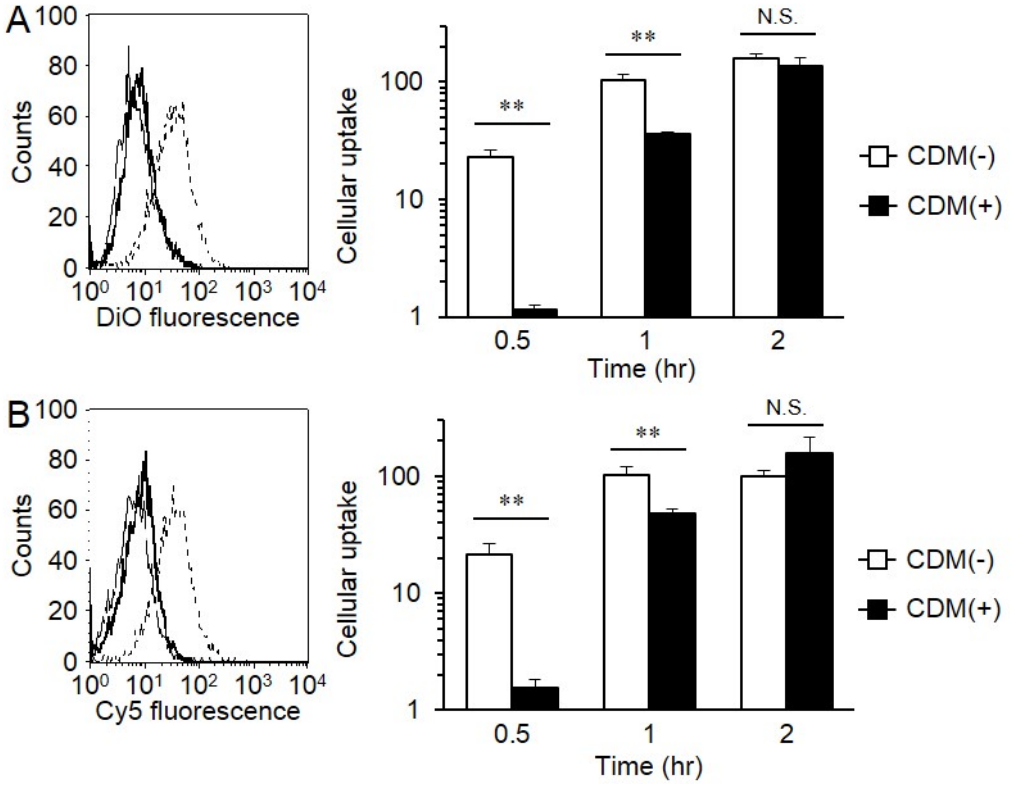

Figure 3 Cellular uptake of the LNPs. Cellular uptake of the LNP lipid (A) and siRNA (B) was measured by measuring the fluorescent intensity of the DiO and Cy5, respectively, using flow cytometry. In the left histogram, Non-treated, CDM(-)-LNP-treated and CDM(+)-LNP-treated samples are represented as solid, dashed and bold solid lines, respectively. n=3. Data are represented as the mean±SD. n=3. **P<0.01 (by unpaired Student's t-test). N.S.: not significant.

To confirm the pH-sensitive detachment of CDM-$_m$PEG$_{2k}$, the recovery of primary amino groups was evaluated by a TNBS assay after the CDM-$_m$PEG$_{2k}$-modified LNPs were incubated at pH 7.4 and 6.0. The recovery rate of the primary amino group was moderate at pH 7.4 and the half-life ($t_{1/2}$) was 45 min (Figure 4A). At 6.0, the $t_{1/2}$ was 6 min, which is 7.5-fold faster compared to pH 7.4 (Figure 4A). The detachment of CDM-$_m$PEG$_{2k}$ from the surface of the LNPs would result in the recovery of fusogenic activity of the LNPs with endosomal membranes due to reduced steric hindrance by the PEG layer (fixed aqueous layer) located on the surface of the LNPs. LNPs that were not modified with CDM-$_m$PEG$_{2k}$ rapidly fused with the anionic liposome which is used as a model endosome [32], reaching a FRET cancellation of approximately 60% (Figure 4B). On the other hand, the LNPs modified with CDM-$_m$PEG$_{2k}$ showed a lower fusogenic

activity (FRET cancellation of approximately 20%) until 2 min after mixing, which results from the stealth function conferred by the PEG layer (Figure 4B). However, a rapid recovery of the fusogenic activity was found after a 2 min incubation period (Figure 4B, arrow). We also confirmed that the fusogenic activity of the CDM-$_m$PEG$_{2k}$-modified LNPs was nearly fully recovered by pre-incubation for 1 hour at pH 6.0 before mixing with anionic liposomes (Figure 4B). These results suggest that the CDM-$_m$PEG$_{2k}$ modification did not inhibit the membrane fusion-mediated endosomal escape of the LNPs after cellular uptake due to the rapid detachment of the PEG layer in the acidic environment.

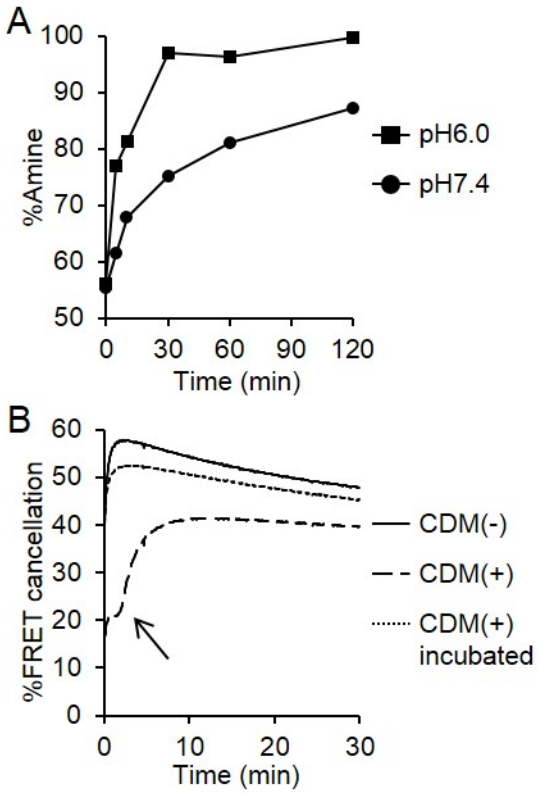

Figure 4 pH-sensitive detachment of CDM-$_m$PEG$_{2k}$. (A) Primary amino groups of the chol-PEG$_{400}$-amine were measured by a TNBS assay after incubation of the CDM-$_m$PEG$_{2k}$-modified LNPs under the indicated conditions. (B) FRET cancellation as an indicator of fusogenicity of the LNPs was monitored after the addition of anionic liposomes. The arrow indicates the recovery of fusogenic activity.

3.3 *In vivo* active targeting

To target hepatocytes, LNPs were modified with0.5 mol% of a trivalent GalNAc ligand (Figure 5A). To evaluate the hepatocyte-targeting ability of the LNPs, mice were intravenously injected with 4 types of of LNPs (GalNAc (±), CDM-$_m$PEG$_{2k}$ (±)). At 60 minutes after injection, the intrahepatic distribution of the LNPs was observed using confocal fluorescent microscopy. Bare LNPs (GalNAc (-), CDM-$_m$PEG$_{2k}$ (-)) were detected on blood vessels of the liver (Figure 5B, upper left) and other organs, including the lungs, heart and kidneys (Figure S2), due to their cationic property (Figure S1A). Modification with CDM-$_m$PEG$_{2k}$ clearly inhibited non-specific adsorption to blood vessels in various organs (Figure S2). However, the LNPs that were modified with CDM-$_m$PEG$_{2k}$ failed to accumulate in hepatocytes due to the absence of the GalNAc ligand (Figure 5B, upper right). Moreover, GalNAc-modified LNPs also failed to accumulate in hepatocytes (Figure 5B, lower left). On the other hand, significant levels of LNPs that were modified with both GalNAc and CDM-$_m$PEG$_{2k}$ accumulated in hepatocytes (Figure 5B, lower right). To confirm that the improvement in intrahepatic distribution results in an increase in gene silencing activity in hepatocytes, siRNA targeting coagulation factor 7 (siF7), a hepatocyte-specific gene, was formulated in the 4 types of LNPs (GalNAc (±), CDM-$_m$PEG$_{2k}$ (±)) and intravenously injected at a dose of 0.5 mg siRNA/kg. Bare LNPs showed approximately a 40% gene silencing under these experimental conditions (Figure 5C). The LNPs with a single modification of GalNAc or CDM-$_m$PEG$_{2k}$ showed a slightly improved activity but the improvement was not statistically significant (Figure 5C). On the other hand, modification with both GalNAc and CDM-$_m$PEG$_{2k}$ resulted in a significant improvement in activity (approximately 90% gene silencing) (Figure 5C), which is reflected by a change in intrahepatic distribution (Figure 5B). To confirm that the uptake of the LNPs that were modified with both GalNAc and CDM-$_m$PEG$_{2k}$ is mediated by the GalNAc/ASGPR pathway, mice were co-injected with galactose, a competitive inhibitor of the interaction between GalNAc and ASGPR. As expected, F7 silencing activity was significantly reduced when galactose was co-injected (Figure S3), suggesting that the uptake of the LNPs by hepatocytes proceeds in a GalNAc-mediated active targeting manner. A significant reduction in F7 activity was observed only after the injection of siF7, but not siRNA targeting the human polo-like kinase 1 (siPLK1), suggesting that the silencing of F7 expression is siRNA sequence-specific (Figure S4A). Moreover, no significant modulation in the expression of several cell-specific marker genes (CD11b, CD31 and CD45) was found, indicating that the developed LNPs are able to induce the specific silencing of the target gene with negligible off-target effects (Figure S4B). No elevation in plasma alanine transaminase (ALT) and aspartate transaminase (AST) levels and no

loss of body weight change was observed at 24 hrs after the injection of the LNPs modified with both GalNAc and CDM-$_m$PEG$_{2k}$ at a dose of 0.5 mg siRNA/kg, which was a highest dose used in this study (Figure S5).

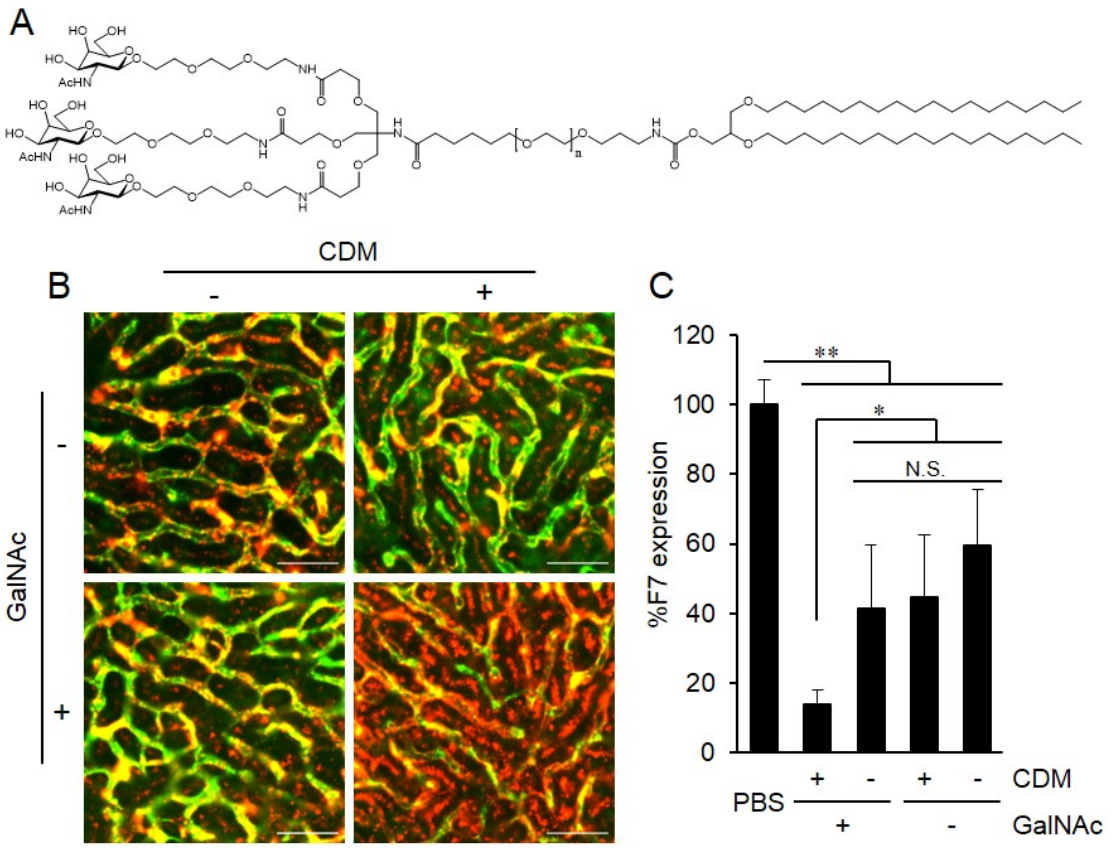

Figure 5 Effect of modifying LNPs with a combination of GalNAc and CDM-$_m$PEG$_{2k}$ on hepatocyte targeting. (A) Chemical structure of the trivalent GalNAc ligand. (B) Intrahepatic distribution of the DiI-labeled LNPs (GalNAc (±), CDM-$_m$PEG$_{2k}$ (±)) 1 hr after intravenous injection at a dose of 0.5 mg siRNA/kg. The LNPs and blood vessels are visualized as red and green, respectively. Bars represent 50 μm. (C) F7 expression 24 hr after intravenous injection of siF7 formulated in the LNPs (GalNAc (±), CDM-$_m$PEG$_{2k}$ (±)) at a dose of 0.5 mg siRNA/kg. Data are represented as the mean±SD. n=3-5. *P<0.05, *P<0.01 (by one-way nrANOVA, followed by SNK test). N.S.: not significant.

The effect of the chemical structure of maleic anhydride was next examined. It has already been revealed that substitution of a carbohydrate at the 2- and 3-positions of the maleic anhydride dramatically improve the acid-sensitive hydrolysis of the amide bond

formed by the reaction of maleic acid and primary amino group [31]. CEM-$_m$PEG$_{2k}$ was synthesized as an analogue of CDM-$_m$PEG$_{2k}$ with higher stability against acid hydrolysis (Figure S6A). Indeed, the rate of detachment of CEM-$_m$PEG$_{2k}$ ($t_{1/2}$ at pH 7.5, 6.0 and 4.0 was over 50 hours, 60 min and 15 min, respectively) from glycine, a simple model compound containing a primary amino group, was clearly lower than that of CDM-$_m$PEG$_{2k}$ ($t_{1/2}$ at pH 7.5 and 6.0 was 30 min and less than 1 min, respectively) (Figure S6B, C). To confirm that the stealth function of the CEM-$_m$PEG$_{2k}$ was improved, the cellular uptake of LNPs modified with CDM- or CEM-$_m$PEG$_{2k}$ was compared *in vitro*. The cellular uptake of both siRNAs (Figure 6A) and LNP lipids (Figure 6B) of the LNPs modified with CEM-$_m$PEG$_{2k}$ was significantly lower, suggesting the superior stealth function of the CEM-$_m$PEG$_{2k}$. Intrahepatic distribution of the GalNAc-modified LNPs with CDM- or CEM-$_m$PEG$_{2k}$ modification was observed. In this experiment, all LNPs were modified with 0.25 mol% GalNAc, which is the optimal density for gene silencing activity in this system (data not shown). As expected, CEM-$_m$PEG$_{2k}$ modification resulted in further improvement of accumulation to hepatocytes (Figure 6C). Reflecting the intrahepatic distribution, CEM-$_m$PEG$_{2k}$-modified LNPs showed 50% effective dose (ED_{50}) of 0.035 mg siRNA/kg, which is approximately 2-fold and 14-fold higher activity compared to the CDM-$_m$PEG$_{2k}$-modified LNPs (ED_{50}: 0.08 mg siRNA/kg) and PEG-unmodified LNPs (ED_{50}: 0.5 mg siRNA/kg) (Figure 6D).

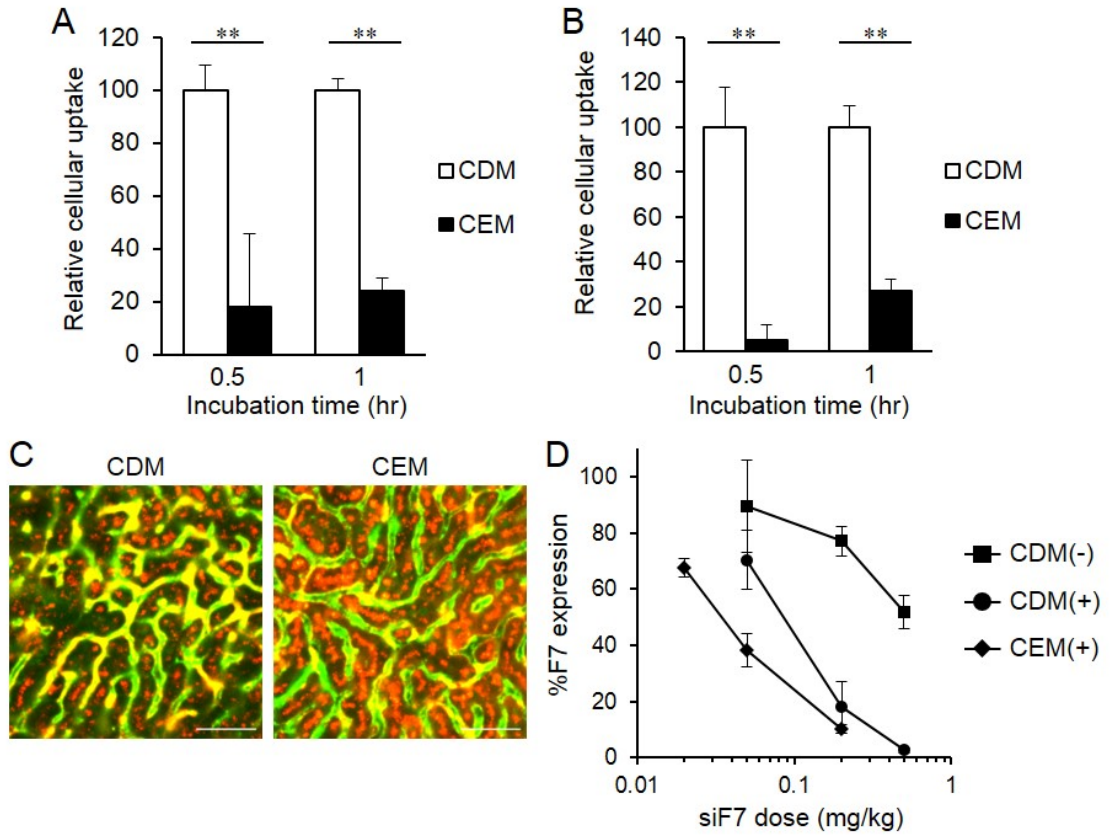

Figure 6 Comparison of CDM-$_m$PEG$_{2k}$ and CEM-$_m$PEG$_{2k}$. (A, B) Cellular uptake of LNPs modified with CDM-$_m$PEG$_{2k}$ or CEM-$_m$PEG$_{2k}$ *in vitro*. The cellular uptake of Cy5-labeled siRNAs (A) and DiO-labeled LNP lipids was measured by flow cytometry. (C) Intrahepatic distribution of the DiI-labeled GalNAc-LNPs modified with CDM-$_m$PEG$_{2k}$ or CEM-$_m$PEG$_{2k}$ 1 hr after intravenous injection at a dose of 0.5 mg siRNA/kg. The LNPs and blood vessels are visualized as red and green, respectively. Bars represent 50 μm. (D) F7 expression 24 hr after an intravenous injection of siF7 formulated in the GalNAc-LNPs at the indicated dose. Data are represented as the mean±SD. n=3.

Discussion

We report herein on the development of a method for the efficient delivery of siRNA to hepatocytes achieved by modifying LNPs with both specific ligands (GalNAc) and PEG via maleic acid amide bonding, which are rapidly hydrolyzed when in a weakly acidic environment. The maleic anhydride-mediated PEGylation conferred to following two important functions: 1) stealth function (minimization of non-specific interaction with biocomponents) in the blood circulation, which results in maximization of ligand-mediated targeting, 2) rapid detachment of the PEG moiety from the surface of the LNPs and re-activation of the fusogenicity of the LNPs in acidified endosomes, which results in enhanced cytosolic delivery of siRNAs (Figure 7).

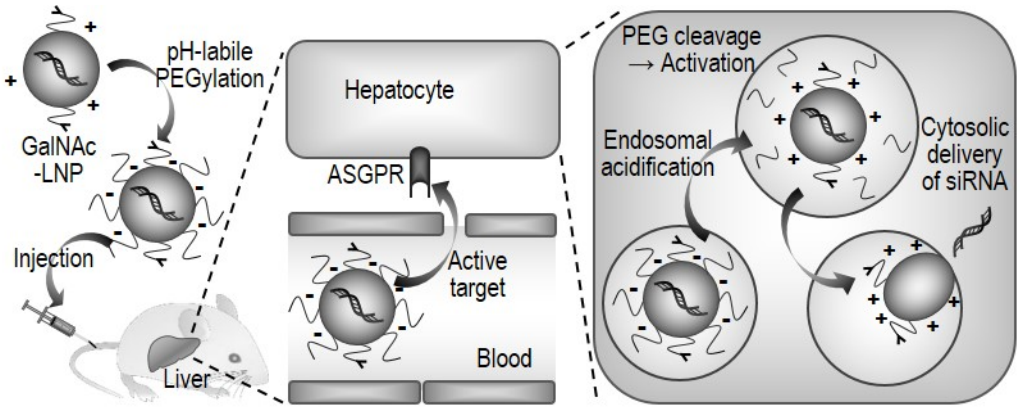

Figure 7 Schematic illustration of the process of the cytosolic delivery of siRNAs by the LNPs. In the blood circulation, the LNPs are biologically shielded by PEGylation. After cellular uptake of the LNPs into hepatocytes via interaction of GalNAc ligands and their receptors, ASGPR, the PEGs are rapidly detached in response to the acidic environment of the endosomes, thus permitting the LNPs to be activated. Efficient membrane fusion between the LNPs and endosomal membranes results in the delivery of the siRNAs to the cytosol.

To modify the LNPs with CDM-$_{m}$PEG$_{2k}$, chol-PEG$_{400}$-amine was inserted as a donor of primary amino groups, which react with maleic anhydride [31]. A spacer, PEG$_{400}$, between the cholesterol (anchor) and primary amino group played an important role in realizing the pH-sensitive detachment of CDM-$_{m}$PEG$_{2k}$ from the surface of the LNPs. Indeed, in the case where phosphatidylethanolamine (PE), instead of chol-PEG$_{400}$-amine, was used as a donor of primary amino group, the hydrolysis rate of the maleic acid amide bond was much slower and the particles were unresponsive to a change in pH (unpublished data). Hydrolysis of the maleic acid amide was achieved via the

nucleophilic attack of the maleic acid carboxylate anion opposite the carbonyl carbon of the maleic acid amide bond. The protonated tertiary amino group (cation) of YSK05 can electrostatically bind to negative carboxylate anions, resulting in the inhibition of the nucleophilic attack for hydrolysis of maleic acid amide bond. Because the primary amino group of PE must be very close to the tertiary amino group of the YSK05, an inhibitory effect would be easy to occur. Under this situation, a spacer, PEG_{400}, was introduced between the hydrophobic anchor and the primary amino group in order to separate carboxylate anion from YSK05 and to minimize the risk of an inhibitory effect. Indeed, a rapid and pH-dependent hydrolysis was observed in our system (Figure 4A). However, to clarify the relationship between spacer length and the inhibitory effect, a detailed examination of the spacer length will be needed.

Reaction of the LNPs with 2.5 equivalents of CDM-$_mPEG_{2k}$ resulted in the consumption of approximately 50% of the primary amino groups (Figure 2B). Because 15 mol% of chol-PEG_{400}-amine was inserted in the LNPs, approximately 7.5 mol% of the CDM-$_mPEG_{2k}$ was modified after reaction with 2.5 equivalents of the CDM-$_mPEG_{2k}$. It has already been clarified that modification of YSK05-based LNPs with 3 mol% $_mPEG_{2k}$ is sufficient to provide a stealth function. In addition, the $t_{1/2}$ for the hydrolysis rate at pH 7.4 was 1 hour, indicating that stealth function would be maintained for approximately 1 hr. Indeed, modifying the LNP with CDM-$_mPEG_{2k}$ resulted in a significant decrease in cellular uptake up to a 1 hour incubation period (Figure 3). Concerning *in vivo*, in a previous study, we found that the $t_{1/2}$ for GalNAc-mediated blood clearance is approximately 25 min, and 1.5 hour is sufficient for the GalNAc-modified LNPs to accumulate in hepatocytes (unpublished data). Therefore, the accumulation of the LNP in hepatocytes was clearly enhanced by modification with both GalNAc and CDM-$_mPEG_{2k}$ (Figure 5B), but it was further enhanced by replacing the CDM with CEM, which shows a lower hydrolysis rate (Figure 6C and S6). Reflected by enhanced accumulation in hepatocytes, gene silencing activity for the same cells was clearly improved (Figure 5C and 6D). This fact suggests that PEGylation of the LNPs through the pH-labile maleic anhydride had no effect on the magnitude of endosomal escape through membrane fusion.

PEGylation of the LNPs through maleic acid amide results, not only in the formation of a thick fixed aqueous layer on the surface of the LNPs, but also in reversing the charge of the LNPs from positive to negative (Figure 2A). Because a positive charge causes non-specific interactions with negatively charged serum proteins and cell surfaces (Figure S2), the characteristics of maleic anhydride, the reversal of charge, is

useful in terms of suppressing the cationic charge of the LNPs in the blood stream and to expand the opportunity for the cationic LNPs to be used for *in vivo* applications.

To our knowledge, this is first report to demonstrate that PEG-modification through maleic anhydride improves the targeting capability and efficiency of the drug delivery of ligand-modified LNPs *in vivo*. Importantly, the fact that the ED_{50} of the optimized LNPs in F7 model mice is a level relevant to clinical applications, suggests that the current strategy has considerable potential for clinical use.

Conclusion

In the present study, we reported on the development of siRNA-loaded LNPs that are modified with both a specific ligand and PEG via maleic acid amide bonding. The rapid and pH-sensitive detachment of PEG moiety and re-activation of fusogenisity was confirmed. *In vivo*, an enhanced efficiency of hepatocyte-targeting and gene silencing activity were confirmed. These lines of the evidence suggest that this strategy, i.e., modifying an LNP with a combination of a specific ligand and maleic anhydride-PEG, can be useful for achieving the efficient LNP-mediated delivery of siRNAs to specific sites.

Acknowledgement

This work was supported by JSPS KAKENHI Grant Number 15K20831. The authors also wish to thank Dr. Milton S. Feather for his helpful advice in writing the English manuscript.

References

[1] S.M. Elbashir, J. Harborth, W. Lendeckel, A. Yalcin, K. Weber, T. Tuschl, Duplexes of 21-nucleotide RNAs mediate RNA interference in cultured mammalian cells, Nature, 411 (2001) 494-498.

[2] A. Fire, S. Xu, M.K. Montgomery, S.A. Kostas, S.E. Driver, C.C. Mello, Potent and specific genetic interference by double-stranded RNA in Caenorhabditis elegans, Nature, 391 (1998) 806-811.

[3] A.L. Klibanov, K. Maruyama, V.P. Torchilin, L. Huang, Amphipathic polyethyleneglycols effectively prolong the circulation time of liposomes, FEBS Lett, 268 (1990) 235-237.

[4] T.M. Allen, C. Hansen, F. Martin, C. Redemann, A. Yau-Young, Liposomes containing synthetic lipid derivatives of poly(ethylene glycol) show prolonged circulation half-lives in vivo, Biochim Biophys Acta, 1066 (1991) 29-36.

[5] P.R. Cullis, A. Chonn, S.C. Semple, Interactions of liposomes and lipid-based carrier systems with blood proteins: Relation to clearance behaviour in vivo, Adv Drug Deliv Rev, 32 (1998) 3-17.

[6] H. Hatakeyama, H. Akita, H. Harashima, A multifunctional envelope type nano device (MEND) for gene delivery to tumours based on the EPR effect: a strategy for overcoming the PEG dilemma, Adv Drug Deliv Rev, 63 (2011) 152-160.

[7] H. Hatakeyama, H. Akita, H. Harashima, The polyethyleneglycol dilemma: advantage and disadvantage of PEGylation of liposomes for systemic genes and nucleic acids delivery to tumors, Biol Pharm Bull, 36 (2013) 892-899.

[8] S. Mishra, P. Webster, M.E. Davis, PEGylation significantly affects cellular uptake and intracellular trafficking of non-viral gene delivery particles, Eur J Cell Biol, 83 (2004) 97-111.

[9] A.A. Kale, V.P. Torchilin, Design, synthesis, and characterization of pH-sensitive PEG-PE conjugates for stimuli-sensitive pharmaceutical nanocarriers: the effect of substitutes at the hydrazone linkage on the ph stability of PEG-PE conjugates, Bioconjug Chem, 18 (2007) 363-370.

[10] G.F. Walker, C. Fella, J. Pelisek, J. Fahrmeir, S. Boeckle, M. Ogris, E. Wagner, Toward synthetic viruses: endosomal pH-triggered deshielding of targeted polyplexes greatly enhances gene transfer in vitro and in vivo, Mol Ther, 11 (2005) 418-425.

[11] X. Guo, J.A. MacKay, F.C. Szoka, Mechanism of pH-triggered collapse of phosphatidylethanolamine liposomes stabilized by an ortho ester polyethyleneglycol lipid, Biophys J, 84 (2003) 1784-1795.

[12] C. Masson, M. Garinot, N. Mignet, B. Wetzer, P. Mailhe, D. Scherman, M. Bessodes, pH-sensitive PEG lipids containing orthoester linkers: new potential tools for nonviral gene

delivery, J Control Release, 99 (2004) 423-434.
[13] V. Knorr, L. Allmendinger, G.F. Walker, F.F. Paintner, E. Wagner, An acetal-based PEGylation reagent for pH-sensitive shielding of DNA polyplexes, Bioconjug Chem, 18 (2007) 1218-1225.
[14] D. Wakebayashi, N. Nishiyama, K. Itaka, K. Miyata, Y. Yamasaki, A. Harada, H. Koyama, Y. Nagasaki, K. Kataoka, Polyion complex micelles of pDNA with acetal-poly(ethylene glycol)-poly(2-(dimethylamino)ethyl methacrylate) block copolymer as the gene carrier system: physicochemical properties of micelles relevant to gene transfection efficacy, Biomacromolecules, 5 (2004) 2128-2136.
[15] Y. Maeda, F. Pittella, T. Nomoto, H. Takemoto, N. Nishiyama, K. Miyata, K. Kataoka, Fine-tuning of charge-conversion polymer structure for efficient endosomal escape of siRNA-loaded calcium phosphate hybrid micelles, Macromol Rapid Commun, 35 (2014) 1211-1215.
[16] S.C. Wong, J.J. Klein, H.L. Hamilton, Q. Chu, C.L. Frey, V.S. Trubetskoy, J. Hegge, D. Wakefield, D.B. Rozema, D.L. Lewis, Co-injection of a targeted, reversibly masked endosomolytic polymer dramatically improves the efficacy of cholesterol-conjugated small interfering RNAs in vivo, Nucleic Acid Ther, 22 (2012) 380-390.
[17] D.B. Rozema, D.L. Lewis, D.H. Wakefield, S.C. Wong, J.J. Klein, P.L. Roesch, S.L. Bertin, T.W. Reppen, Q. Chu, A.V. Blokhin, J.E. Hagstrom, J.A. Wolff, Dynamic PolyConjugates for targeted in vivo delivery of siRNA to hepatocytes, Proc Natl Acad Sci U S A, 104 (2007) 12982-12987.
[18] N. Yamamoto, Y. Sato, T. Munakata, M. Kakuni, C. Tateno, T. Sanada, Y. Hirata, S. Murakami, Y. Tanaka, K. Chayama, H. Hatakeyama, M. Hyodo, H. Harashima, M. Kohara, Novel pH-sensitive multifunctional envelope-type nanodevice for siRNA-based treatments for chronic HBV infection, J Hepatol, 64 (2016) 547-555.
[19] T.S. Zimmermann, A.C. Lee, A. Akinc, B. Bramlage, D. Bumcrot, M.N. Fedoruk, J. Harborth, J.A. Heyes, L.B. Jeffs, M. John, A.D. Judge, K. Lam, K. McClintock, L.V. Nechev, L.R. Palmer, T. Racie, I. Röhl, S. Seiffert, S. Shanmugam, V. Sood, J. Soutschek, I. Toudjarska, A.J. Wheat, E. Yaworski, W. Zedalis, V. Koteliansky, M. Manoharan, H.P. Vornlocher, I. MacLachlan, RNAi-mediated gene silencing in non-human primates, Nature, 441 (2006) 111-114.
[20] Y.Y. Tam, S. Chen, P.R. Cullis, Advances in Lipid Nanoparticles for siRNA Delivery, Pharmaceutics, 5 (2013) 498-507.
[21] F. Leuschner, P. Dutta, R. Gorbatov, T.I. Novobrantseva, J.S. Donahoe, G. Courties, K.M. Lee, J.I. Kim, J.F. Markmann, B. Marinelli, P. Panizzi, W.W. Lee, Y. Iwamoto, S. Milstein, H. Epstein-Barash, W. Cantley, J. Wong, V. Cortez-Retamozo, A. Newton, K. Love, P. Libby, M.J.

Pittet, F.K. Swirski, V. Koteliansky, R. Langer, R. Weissleder, D.G. Anderson, M. Nahrendorf, Therapeutic siRNA silencing in inflammatory monocytes in mice, Nat Biotechnol, 29 (2011) 1005-1010.

[22] S. Warashina, T. Nakamura, Y. Sato, Y. Fujiwara, M. Hyodo, H. Hatakeyama, H. Harashima, A lipid nanoparticle for the efficient delivery of siRNA to dendritic cells, J Control Release, 225 (2016) 183-191.

[23] S.C. Semple, A. Akinc, J. Chen, A.P. Sandhu, B.L. Mui, C.K. Cho, D.W. Sah, D. Stebbing, E.J. Crosley, E. Yaworski, I.M. Hafez, J.R. Dorkin, J. Qin, K. Lam, K.G. Rajeev, K.F. Wong, L.B. Jeffs, L. Nechev, M.L. Eisenhardt, M. Jayaraman, M. Kazem, M.A. Maier, M. Srinivasulu, M.J. Weinstein, Q. Chen, R. Alvarez, S.A. Barros, S. De, S.K. Klimuk, T. Borland, V. Kosovrasti, W.L. Cantley, Y.K. Tam, M. Manoharan, M.A. Ciufolini, M.A. Tracy, A. de Fougerolles, I. MacLachlan, P.R. Cullis, T.D. Madden, M.J. Hope, Rational design of cationic lipids for siRNA delivery, Nat Biotechnol, 28 (2010) 172-176.

[24] M. Jayaraman, S.M. Ansell, B.L. Mui, Y.K. Tam, J. Chen, X. Du, D. Butler, L. Eltepu, S. Matsuda, J.K. Narayanannair, K.G. Rajeev, I.M. Hafez, A. Akinc, M.A. Maier, M.A. Tracy, P.R. Cullis, T.D. Madden, M. Manoharan, M.J. Hope, Maximizing the potency of siRNA lipid nanoparticles for hepatic gene silencing in vivo, Angew Chem Int Ed Engl, 51 (2012) 8529-8533.

[25] A. Akinc, A. Zumbuehl, M. Goldberg, E.S. Leshchiner, V. Busini, N. Hossain, S.A. Bacallado, D.N. Nguyen, J. Fuller, R. Alvarez, A. Borodovsky, T. Borland, R. Constien, A. de Fougerolles, J.R. Dorkin, K. Narayanannair Jayaprakash, M. Jayaraman, M. John, V. Koteliansky, M. Manoharan, L. Nechev, J. Qin, T. Racie, D. Raitcheva, K.G. Rajeev, D.W. Sah, J. Soutschek, I. Toudjarska, H.P. Vornlocher, T.S. Zimmermann, R. Langer, D.G. Anderson, A combinatorial library of lipid-like materials for delivery of RNAi therapeutics, Nat Biotechnol, 26 (2008) 561-569.

[26] K.T. Love, K.P. Mahon, C.G. Levins, K.A. Whitehead, W. Querbes, J.R. Dorkin, J. Qin, W. Cantley, L.L. Qin, T. Racie, M. Frank-Kamenetsky, K.N. Yip, R. Alvarez, D.W. Sah, A. de Fougerolles, K. Fitzgerald, V. Koteliansky, A. Akinc, R. Langer, D.G. Anderson, Lipid-like materials for low-dose, in vivo gene silencing, Proc Natl Acad Sci U S A, 107 (2010) 1864-1869.

[27] Y. Dong, K.T. Love, J.R. Dorkin, S. Sirirungruang, Y. Zhang, D. Chen, R.L. Bogorad, H. Yin, Y. Chen, A.J. Vegas, C.A. Alabi, G. Sahay, K.T. Olejnik, W. Wang, A. Schroeder, A.K. Lytton-Jean, D.J. Siegwart, A. Akinc, C. Barnes, S.A. Barros, M. Carioto, K. Fitzgerald, J. Hettinger, V. Kumar, T.I. Novobrantseva, J. Qin, W. Querbes, V. Koteliansky, R. Langer, D.G. Anderson, Lipopeptide nanoparticles for potent and selective siRNA delivery in rodents and nonhuman primates, Proc Natl Acad Sci U S A, 111 (2014) 3955-3960.

[28] J.K. Nair, J.L. Willoughby, A. Chan, K. Charisse, M.R. Alam, Q. Wang, M. Hoekstra, P. Kandasamy, A.V. Kel'in, S. Milstein, N. Taneja, J. O'Shea, S. Shaikh, L. Zhang, R.J. van der Sluis, M.E. Jung, A. Akinc, R. Hutabarat, S. Kuchimanchi, K. Fitzgerald, T. Zimmermann, T.J. van Berkel, M.A. Maier, K.G. Rajeev, M. Manoharan, Multivalent N-acetylgalactosamine-conjugated siRNA localizes in hepatocytes and elicits robust RNAi-mediated gene silencing, J Am Chem Soc, 136 (2014) 16958-16961.

[29] A. Akinc, W. Querbes, S. De, J. Qin, M. Frank-Kamenetsky, K.N. Jayaprakash, M. Jayaraman, K.G. Rajeev, W.L. Cantley, J.R. Dorkin, J.S. Butler, L. Qin, T. Racie, A. Sprague, E. Fava, A. Zeigerer, M.J. Hope, M. Zerial, D.W. Sah, K. Fitzgerald, M.A. Tracy, M. Manoharan, V. Koteliansky, A. Fougerolles, M.A. Maier, Targeted delivery of RNAi therapeutics with endogenous and exogenous ligand-based mechanisms, Mol Ther, 18 (2010) 1357-1364.

[30] Y. Sato, H. Hatakeyama, Y. Sakurai, M. Hyodo, H. Akita, H. Harashima, A pH-sensitive cationic lipid facilitates the delivery of liposomal siRNA and gene silencing activity in vitro and in vivo, J Control Release, 163 (2012) 267-276.

[31] D.B. Rozema, K. Ekena, D.L. Lewis, A.G. Loomis, J.A. Wolff, Endosomolysis by masking of a membrane-active agent (EMMA) for cytoplasmic release of macromolecules, Bioconjug Chem, 14 (2003) 51-57.

[32] Y. Zhang, L. Arrington, D. Boardman, J. Davis, Y. Xu, K. DiFelice, S. Stirdivant, W. Wang, B. Budzik, J. Bawiec, J. Deng, G. Beutner, D. Seifried, M. Stanton, M. Gindy, A. Leone, The development of an in vitro assay to screen lipid based nanoparticles for siRNA delivery, J Control Release, 174 (2014) 7-14.

Supplementary Information

pH-labile PEGylation of siRNA-loaded lipid nanoparticle improves active targeting and gene silencing activity in hepatocytes

*Kazuki Hashiba,† Yusuke Sato,† Hideyoshi Harashima**

Faculty of Pharmaceutical Sciences, Hokkaido University, Kita 12 Nishi 6, Kita-ku, Sapporo 060-0812, Japan

†These authors are contributed equally to this work.

A General Information

^{1}H NMR spectra were obtained on a JEOL ECA500, ECX400P or ECS400 instrument, with tetramethylsilane as the internal standard (0 ppm). The following abbreviations were used to express multiplets: s = singlet; d = doublet; t = triplet; m = multiplet. ^{1}H NMR cheimcal shifts are reported in ppm on the sigma scale downfield from tetramethylsilane. All reactions were monitored by thin-layer chromatography on pre-coated TLC plates (Millipore), visualization was achieved by using phosphomolybdic acid stain or *p*-anisaldehyde stain. The products were purified by flash column chromatography on silica gel or an automated Teledyne ISCO combiflash Rf chromatography system. All ordinary chemicals were purchased from commercial sources and were used without further purification.

Methods

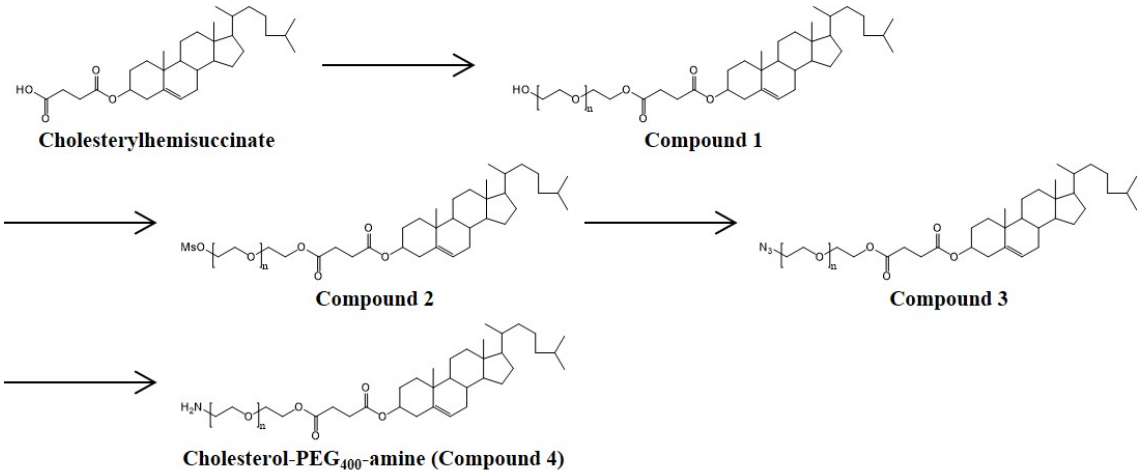

Synthesis of cholesterol-PEG$_{400}$-OH (1). Cholesterylhemisuccinate (2.43 g, 5.00 mmol) was dissolved in anhydrous dichloromethane (DCM) (20 mL), and poltethyleneglycol 400 (PEG$_{400}$) (10.0 g, 25.0 mmol), 4-dimethylaminopyridine (DMAP) (61.1 mg, 0.50 mmol), diisopropylethylamine (DIPEA) (1.22 mL, 7.00 mmol) and 1-(3- Dimethylaminopropyl)-3-ethylcarbodiimide hydrochloride (EDCI) (1.15 g, 6.00 mmol) were added to this solution. The reaction mixture was stirred overnight at ambient temperature. The solvents were removed *in vacuo* and the residue was then diluted with EtOAc (50 mL) and the resulting solution was washed with water (50 mL) and brine (50 mL). The organic phase was dried over Na_2SO_4 and the solvents were removed *in vacuo*. The crude product was chromatographed on silica gel (SiO_2, DCM/MeOH) to give **cholesterol-PEG$_{400}$-OH** as a colorless viscous oil. ^{1}H NMR (400 MHz, $CDCl_3$) δ: 5.36 (1H, d), 4.55-4.65 (1H, m), 4.23 (2H, t), 3.58-3.73 (32H, m), 2.55-2.68 (4H, m), 2.30 (2H, d), 0.83-2.04 (39H, m), 0.66 (3H, s).

Synthesis of cholesterol-PEG$_{400}$-OMs (2). DIPEA (357 μL, 2.10 mmol), DMAP (18.3 mg, 0.15 mmol), methanesulfonyl chloride (139 μL, 1.80 mmol) were successively added to compound **1** (1.01 g, 1.51 mmol) in 10 mL of anhydrous DCM. The reaction mixture was stirred overnight at room temperature. Evaporation of the solvent resulted in a yellowish oily residue. The residue was diluted with EtOAc (50 mL) and the resulting solution was washed with water (50 mL) and brine (50 mL). The organic phase was dried over Na_2SO_4 and the solvents were removed *in vacuo*. The crude product was purified by flash chromatography (SiO_2, DCM/MeOH) to give **cholesterol-PEG$_{400}$-OMs** as a pale yellow oil.

Synthesis of cholesterol-PEG$_{400}$-N$_3$ (3). Sodium azide (488 mg, 7.50 mmol) was added to compound **2** (1.51 mmol) in 5 mL of anhydrous N,N-dimethylformamide. The reaction mixture was stirred overnight at 100°C. The mixture was cooled to room temperature, diluted with EtOAc (50 mL) and the resulting solution was washed with water (50 mL) and brine (50 mL). The organic phase was dried over Na_2SO_4 and the solvents were removed *in vacuo*. The crude product was purified by flash chromatography (SiO_2, DCM/MeOH) to give **cholesterol-PEG$_{400}$-N$_3$** as a pale yellow wax. ^{1}H NMR (400 MHz, $CDCl_3$) δ: 5.35 (1H, d), 4.55-4.65 (1H, m), 4.23 (2H, t), 3.58-3.75 (30H, m), 3.38 (2H, t), 2.55-2.68 (4H, m), 2.30 (2H, d), 0.83-2.04 (39H, m), 0.66 (3H, s).

Synthesis of cholesterol-PEG$_{400}$-amine (4). Triphenylphosphine (315 mg, 1.20 mmol) was added to compound 3 (937 mg, 1.05 mmol) in 10 mL of anhydrous tetrahydrofuran (THF). The reaction mixture was stirred for 2 days at room temperature. Water (21.5 μL, 1.20 mmol) was added to the reaction mixture. The reaction mixture was stirred overnight at room temperature. Trifluoroacetic acid (TFA) (91.8 μL, 1.20 mmol) was added to the reaction mixture. Evaporation of the solvent resulted in a yellowish oily residue. The oily residue was purified by flash chromatography (SiO_2, DCM/MeOH) to give 616 mg (67.6% yield) of **cholesterol-PEG$_{400}$-amine** as a pale yellow wax. ^{1}H NMR (400 MHz, $CDCl_3$) δ: 5.34 (1H, d), 4.55-4.65 (1H, m), 4.22 (2H, t), 3.50-3.80 (31H, m), 2.89 (2H, t), 2.55-2.68 (4H, m), 2.30 (2H, d), 0.83-2.04 (39H, m), 0.65 (3H, s).

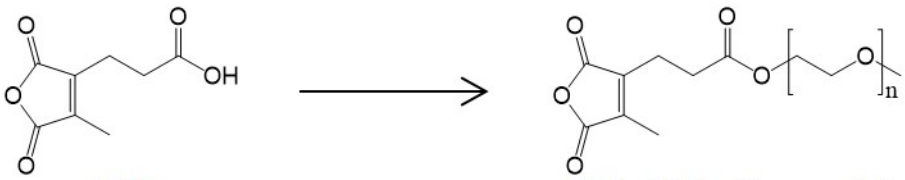

CDM CDM-$_m$PEG$_{2k}$ (Compound 5)

Synthesis of CDM-$_m$PEG$_{2k}$ (5). DMF (3 μL) and oxalyl chloride (429 μL, 5.0 mmol) was successively added to 3-(4-Methyl-2,5-dioxo-2,5-dihydrofuran-3-yl)propanoic acid (CDM) (92.1 mg, 0.50 mmol) in 10 mL of anhydrous DCM. The reaction mixture was stirred overnight at room temperature. Evaporation of the solvent resulted in a yellowish oily residue. This was used for the next reaction without further purification. Methoxypolyethyleneglycol 2000 ($_m$PEG$_{2k}$) (1.10 g, 0.55 mmol) and pyridine (80.5 μL, 1.0 mmol) were successively added to the above crude product in 3 mL of anhydrous DCM. The reaction mixture was stirred overnight at room temperature. Evaporation of the solvent resulted in a yellowish waxy residue. The waxy residue was purified by flash chromatography (C18, H_2O/acetonitrile, 0.1%TFA) to give 848 mg (78.4% yield) of **CDM-$_m$PEG$_{2k}$** as a pale yellow wax. ^{1}H NMR (400 MHz, D_2O) δ: 4.20 (2H, t), 3.43-3.85 (180H, m), 3.36 (3H, s), 2.73 (4H, m), 2.11 (3H, s).

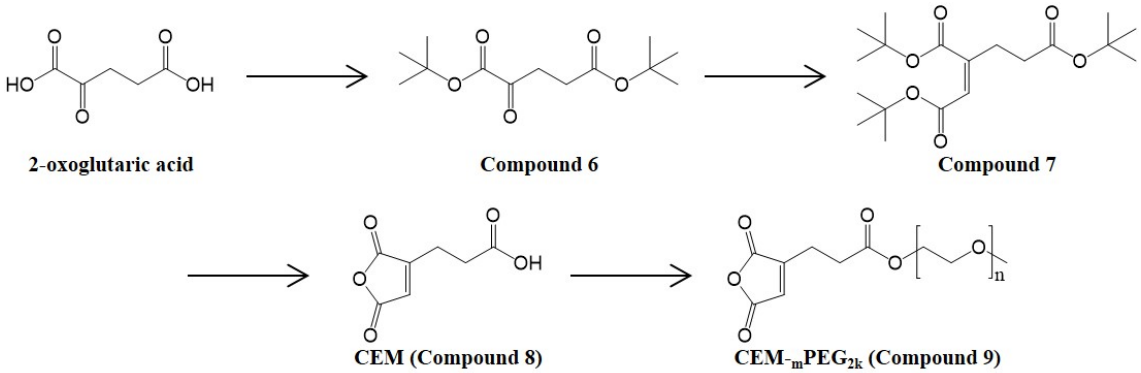

2-oxoglutaric acid Compound 6 Compound 7 CEM (Compound 8) CEM-$_m$PEG$_{2k}$ (Compound 9)

Synthesis of di-*tert*-butyl-2-oxopentanedioate (6). Isobutene (ca. 8% in DCM, 250 mL) and H_2SO_4 (2 mL) was successively added to 2-oxoglutaric acid (7.31 g, 50 mmol). The reaction mixture was stirred for 4 days at room temperature. The solvent was removed by an infusion of argon gas and then *in vacuo*. The residue was diluted with AcOEt (100 mL) and the resulting solution was washed with sat. $NaHCO_3$aq. (2×100 mL) and brine (100 mL). The organic phase was dried over Na_2SO_4 and the solvents were removed *in vacuo*. The crude product was purified by flash chromatography (SiO_2, hexane/AcOEt) to give 6.86. g (53.2% yield) of **di-*tert*-butyl-2-oxopentanedioate** as a pale yellow oil. ^{1}H NMR (400 MHz, $CDCl_3$) δ: 3.03 (2H, t), 2.53 (2H, t), 1.52 (9H, s), 1.42 (9H, s).

Synthesis of tri-*tert*-butyl (Z)-but-1-ene-1,2,4-tricarboxylate (7). *tert*-Butyl 2-(di-*tert*-butoxyphosphoryl)acetate (2.83 mL, 12.0 mmol) was added dropwise to a stirred, ice-cooled suspension of sodium hydride (NaH) (440 mg, 11 mmol, 60%) in 10 mL of anhydrous DCM. The reaction mixture was stirred for 30 min on ice. Compound **6** (2.58 g, 10.0 mmol) was added to the stirred, ice-cooled reaction mixture. The reaction mixture was stirred for 5 hr on ice. The reaction mixture was diluted with AcOEt (50 mL) and the resdulting solution was washed with sat. $NaHCO_3$aq. (2×100 mL) and brine (100 mL) and brine (100 mL). The organic phase was dried over Na_2SO_4 and the solvents were removed *in vacuo*. The crude product was purified by flash chromatography (SiO_2, hexane/AcOEt) to give 1.85 g (51.9% yield) of **tri-*tert*-butyl (Z)-but-1-ene-1,2,4-tricarboxylate** as a colorless oil. ^{1}H NMR (400 MHz, $CDCl_3$) δ: 5.70 (1H, s), 2.56 (2H, t), 2.41 (2H, t), 1.52 (9H, 2), 1.45 (9H, s), 1.42 (9H, s).

Synthesis of 3-(2,5-dioxo-2,5-dihydrofuran-3-yl)propanoic acid (CEM) (8). Formic acid (88%, 70 mL) was added to compound **7** (2.54 g, 7.13 mmol). The reaction mixture was stirred overnight at room temperature. The solvents were removed *in vacuo*. The residue was purified by flash chromatography (C18, H_2O/acetonitrile, 0.1%TFA) to give 792 mg (65.4% yield) of **CEM** as a white powder. ^{1}H NMR (400 MHz, D_2O) δ: 5.82 (1H, s), 2.47-2.58 (4H, m).

Synthesis of CEM-$_m$PEG$_{2k}$ (9). DMF (6 μL) and oxalyl chloride (1.72 mL, 20.0 mmol) was successively added to compound **8** (CEM) (340 mg, 2.0 mmol) in 30 mL of anhydrous DCM. The reaction mixture was stirred overnight at room temperature. Evaporation of the solvent resulted in a yellowish oily residue. This was used for next reaction without further purification. Methoxypolyethyleneglycol 2000 ($_m$PEG$_{2k}$) (4.50 g, 2.25 mmol) and pyridine (242 μL, 3.0 mmol) were successively added the residue in 10 mL of anhydrous DCM. The reaction mixture was stirred for 4 hr at room temperature. Evaporation of the solvent resulted in a yellowish waxy residue. The waxy residue was purified by flash chromatography (C18, H_2O/acetonitrile, 0.1%TFA) to give 402 mg (9.3% yield) of **CEM-$_m$PEG$_{2k}$** as a white wax. ^{1}H NMR (400 MHz, D_2O) δ: 5.82 (1H, s), 3.43-3.85 (180H, m), 3.36 (3H, s), 2.71 (4H, m).

Gene silencing activity *in vitro*

HeLa cells stably expressing Firefly and Renilla luciferase (HeLa-dluc) were cultured in cell-culture dishes (Corning) containing DMEM supplemented with 10% FBS,

penicillin (100 U/mL), streptomycin (100 μg/mL) and G418 (0.4 mg/mL) at 37˚C in 5% CO_2. Hela-dluc cells were seeded at 2.5-3.0×10^4 cells per well in 24-well plates in growth medium 24 h prior to transfection. LNP were diluted with DMEM containing 10% FBS to the indicated siGL4 concentration and transfected after removing spent media by aspiration. Hela-dluc cells were washed with PBS(-) 24 h after transfection and Firefly and Renilla luciferase activity were analyzed using Dual-Glo assay (Promega, WI, USA) according to the manufacturer's protocol. Luminescence was measured using a luminometer (Luminescenser-PSN, Atto, Tokyo, Japan) and normalized to that of control cells that had been transfected with DMEM not containing siGL4.

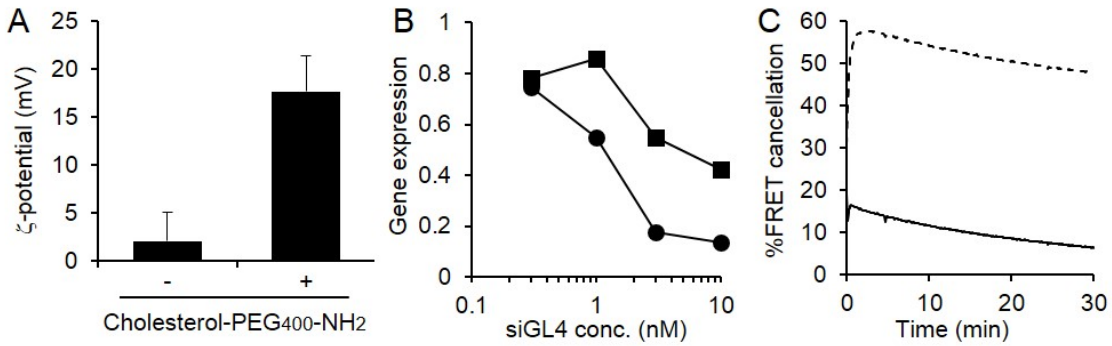

Figure S1. Effect of cholesterol-PEG_{400}-amine modificaion. (A) ζ-potentials of cholesterol-PEG_{400}-amine-modified and unmodified LNPs. n=3 (B) GL4 gene expression of HeLa-dluc cells 24 hr after transfection of siGL4 formulated in the LNPs. Circle and squear represents the cholesterol-PEG_{400}-amine-modified and unmodified LNPs, respectively. n=2. (C) FRET cancellation as ah indicator of fusogenicity of the LNPs. Solid and dashed lines represent the cholesterol-PEG_{400} amine-unmodified and modified LNPs, respectively. n=2.

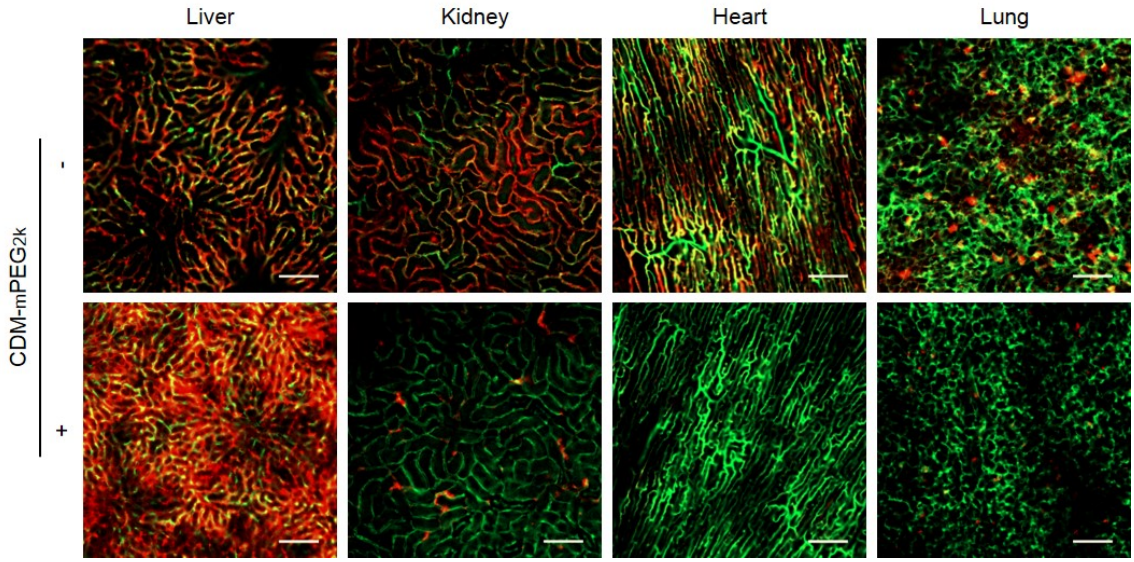

Figure S2. Biodistribution of the LNPs with or without CDM-$_m$PEG$_{2k}$ modification. The indicated tissues were collected 15 min after the intravenous injection of the DiI-labeled LNPs and observed by confocal laser-scaning microscopy. The LNPs and blood vessels are visualized as red and green, respectively. Bars represent 100 μm.

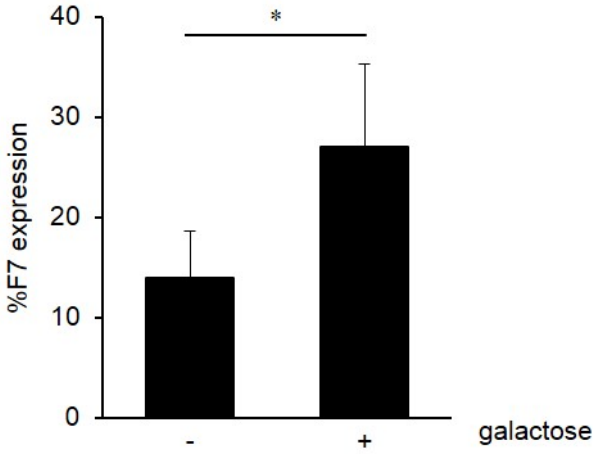

Figure S3. Confirmation of ASGPR-mediated gene silencing. Plasma F7 activity was measured 24 hrs after the injection of siF7 formulated in the LNPs with GalNAc and CDM-$_m$PEG$_{2k}$ at a dose of 0.1 mg/kg. Mice were injected with 14 mg of galactose for ASGPR inhibition. n=4. **P<0.05 (by unpaired Student's *t*-test).

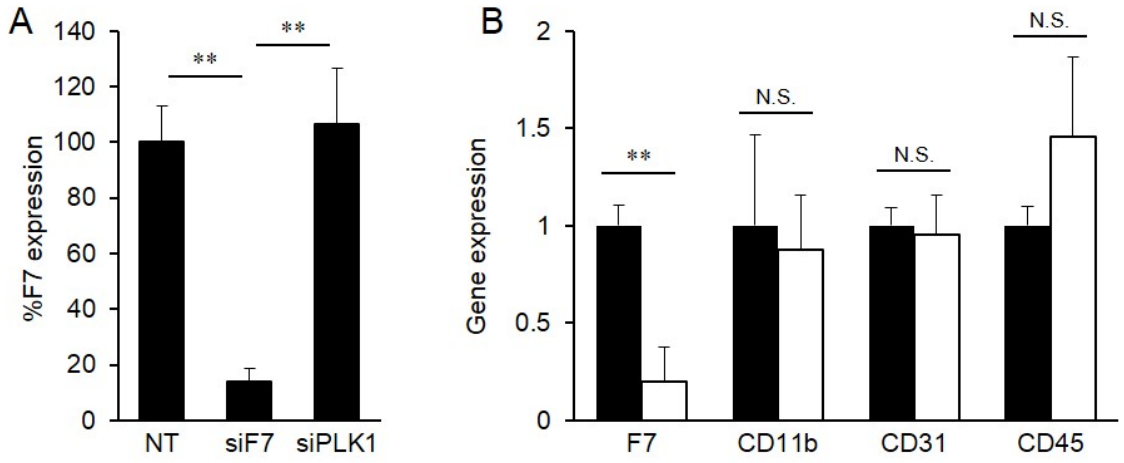

Figure S4. Confirmation of specificity of F7 gene silencing *in vivo*. (A) Plasma F7 activity was measured 24 hrs after injection of siF7 or siPLK1 formulated in the LNPs with GalNAc and CDM-$_m$PEG$_{2k}$ at a dose of 0.1 mg/kg. n=3-4. **P<0.01 (by one-way nrANOVA, followed by SNK test). (B) Expression of mRNA regarding several marker genes in liver tissue was quantified 24 hrs after injection of the siF7 formulated in the LNPs with GalNAc and CDM-$_m$PEG$_{2k}$ at a dose of 0.1 mg/kg. n=3. **P<0.01 (by unpaired Student's *t*-test). N.S.: not significant.

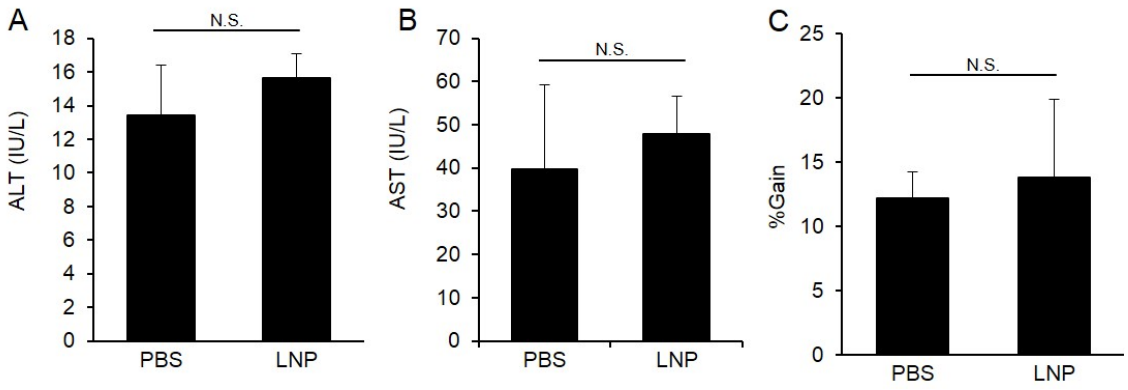

Figure S5. Toxicity of the LNPs. Mice were injected with LNPs modified with both GalNAc and CDM-$_m$PEG$_{2k}$ at a dose of 0.1 mg siRNA/kg. Plasma (A) ALT, (B) AST and (C) body weights were measured 24 hrs after the injection. n=3. N.S.: not significant.

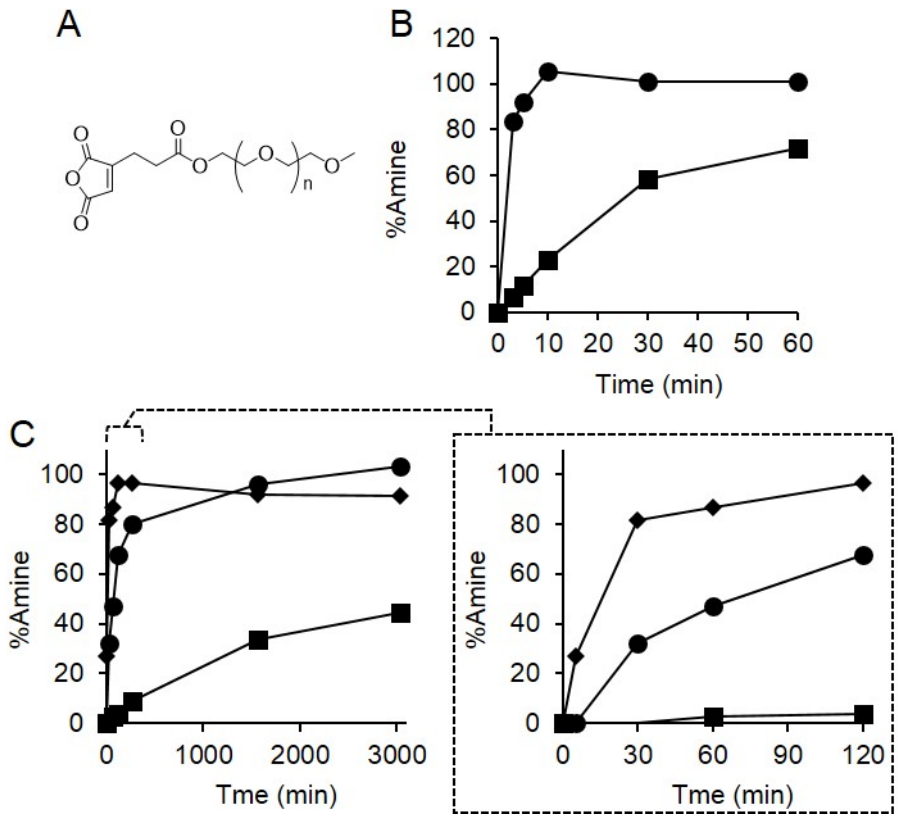

Figure S6. Comparison of CDM- and CEM-$_m$PEG$_{2k}$. (A) Chemical structure of the CEM-$_m$PEG$_{2k}$. (B, C) Rate of detachment of CDM-$_m$PEG$_{2k}$ (B) and CEM-$_m$PEG$_{2k}$ (C) from glycine, a simple model compound containing a primary amino group. Squares, circles and diamonds represent pH7.5, 6.0 and 4.0, respectively. n=2-3.